

This is a repository copy of *Optical characteristics of radially-polarised twisted light*.

White Rose Research Online URL for this paper:

<https://eprints.whiterose.ac.uk/id/eprint/201186/>

Version: Accepted Version

Article:

Koksal, K., Babiker, M. orcid.org/0000-0003-0659-5247 and Lembessis, V. E. (2023) Optical characteristics of radially-polarised twisted light. *Journal of Optics (United Kingdom)*. 065501. ISSN: 2040-8986

<https://doi.org/10.1088/2040-8986/accbd1>

Reuse

This article is distributed under the terms of the Creative Commons Attribution (CC BY) licence. This licence allows you to distribute, remix, tweak, and build upon the work, even commercially, as long as you credit the authors for the original work. More information and the full terms of the licence here:

<https://creativecommons.org/licenses/>

Takedown

If you consider content in White Rose Research Online to be in breach of UK law, please notify us by emailing eprints@whiterose.ac.uk including the URL of the record and the reason for the withdrawal request.

Optical characteristics of radially-polarised twisted light

K. Koksall^{1,2}, M. Babiker¹

¹*Department of Physics, University of York, YO10 5DD, UK and*

²*Physics Department, Bitlis Eren University, Bitlis 13000, Turkey*

V. E. Lembessis³

³*Quantum Technology Group, Department of Physics and Astronomy,
College of Science, King Saud University, Riyadh 11451, Saudi Arabia*

(Dated: June 22, 2023)

Recent work has confirmed that radially-polarised optical modes, specifically those endowed with helical wave fronts can now be routinely generated in the laboratory. Here we show that such a paraxial mode carries only an axial total optical angular momentum (AM) $\tilde{J}_z = \ell \mathcal{L}_0$ where ℓ is the winding number and \mathcal{L}_0 is a constant. This mode, however, is shown to have zero spin angular momentum (SAM), so it is endowed only with orbital angular momentum (OAM) and no SAM. The helicity is found to be proportional to ℓ , hence this kind of mode displays chirality. When applied to a Laguerre-Gaussian (LG) mode our treatment leads to a total helicity equal to $(\ell/|\ell|)\mathcal{Q}$, where \mathcal{Q} is the action constant. The factor $(\ell/|\ell|) = \pm 1$, depends on the sign, not the magnitude of ℓ and so the result holds for any radially-polarised LG mode however large the magnitude of its winding number ℓ is. The magnitude of the action constant \mathcal{Q} and hence the helicity are diminished for all such LG modes of large beam waist w_0 .

INTRODUCTION

A great deal of work has already been carried out on twisted light and on exploring its interaction with matter [1–6], including atoms and molecules [7]. Cylindrical twisted light modes come in a variety of forms, depending on how they are generated, but all the familiar forms are commonly characterised by the ubiquitous azimuthal phase factor $e^{i\ell\phi}$ in the generic amplitude function, which we denote by \mathcal{F} . Here ℓ is the winding number and ϕ is the azimuthal angle in cylindrical polar coordinates. Wave polarisation is an additional, equally significant, ingredient adding another layer of complexity to twisted light. Familiar wave polarisation types include linear, circular and elliptical, together with superpositions of those when dealing with interfering modes. Other forms of polarisation are generally referred to as vector modes [8] and include, in particular, the radial and azimuthal polarisations and superpositions. Here we are concerned with radially-polarised modes which, since their generation in laser oscillations [9, 10], have been of considerable interest and, especially so, more recently in the context of twisted light [11]. A prominent characteristic of radially-polarised light is that its beams focus into very small waists compared with uniformly-polarised modes [12–15]. It is well-known, however, that pure radially-polarised optical vortex modes have no phase dependence and so they do not have the usual helical wavefronts which are characteristic of optical vortex modes. Recent research, however, has succeeded in endowing the usual none-rotating radially-polarised modes with phase properties $e^{i\ell\Phi}$, rendering them like other vortex modes. It is this type of radially-polarised modes we are concerned with in this paper.

However, as far as we know, the optical properties of such radially-polarised twisted light have not yet been explored. In particular, there is need to determine the energy-momentum, spin angular momentum, total angular momentum and the helicity and chirality of such modes. The purpose of this article is to set out the formalism needed to determine these properties. We focus on the paraxial regime and aim to evaluate the properties to leading order. The main ingredients of the formalism emphasise the need to ensure that the electromagnetic fields include the longitudinal components for both the electric and magnetic fields and that Maxwell's equations are satisfied. This means that once the magnetic field format is determined, the electric field follows by application of Maxwell's curl equation and vice versa the magnetic field follows from the electric field by application of the second curl equation.

We aim to deal with monochromatic paraxial radially-polarised vortex modes, mainly without specifying the kind of vortex mode and consider the cycle-averaged properties. These are the spin angular momentum, the orbital angular momentum and the helicity and chirality. We aim to show how the general results for an arbitrary optical vortex lead to well-defined properties when the type of vortex mode is specified and we evaluate the properties for the special case of a Laguerre-Gaussian optical vortex mode.

We find that, typically any radially-polarised paraxial twisted optical mode is endowed with a total angular momentum (AM) which is only ℓ quantised where ℓ is the winding number and it always has zero spin angular momentum (SAM), so it just carries orbital angular momentum (OAM) and no SAM. The optical helicity is shown to be proportional to ℓ , confirming that radially-polarised modes display chirality as it changes sign with the sign

of the winding number ℓ . This is a manifestation of geometrical chirality arising from the geometrical structure of the beam [16]. Our general results are then applied to the case of a Laguerre-Gaussian (LG) mode and we find that the total helicity is equal to $(\ell/|\ell|)Q$, where Q is the action constant, while the factor $(\ell/|\ell|) = \pm 1$ is the Hopf index of the radially-polarised LG mode. We show that this result is applicable to any radially-polarised LG mode however large the magnitude of its winding number ℓ is. We also find that the helicity is diminished for all such LG modes of large beam waist w_0 .

RADIALLY-POLARISED VORTEX FIELDS

Radially-polarised optical vortex modes are routinely producible using commercially available devices in the form of polarisation converters [17]; [18]. Such modes, typically of the Laguerre-Gaussian type, have also been created in the laboratory [19–21]. These reports indicate that such modes are endowed with the phase function $e^{i\ell\phi}$, with the magnitude of the winding number as large as $|\ell|$ up to 200 [22]. One of the methods for generation of a rotating radially-polarised mode involves passing a linearly polarised optical vortex mode through a polarisation converter, which changes the polarisation from \hat{x} to a radial polarisation $\hat{\rho}$. The radially-polarised mode emerging from the polarisation converter keeps its vortex amplitude function \mathcal{U} of the linearly polarised mode incident on the converter but it acquires the polarisation $\hat{\rho}$. Another method involves creating the radially-polarised mode first then passing this mode through a spiral phase plate with a step that adds an integral number ℓ of 2π per turn. This method too keeps the radial polarization and adds an azimuthal phase.

In cylindrical coordinates the electric and magnetic fields of a radially-polarised paraxial twisted light mode created as described above are derivable from a vector potential in the form

$$\mathbf{A}(\rho, \phi, z) = \hat{\rho} \mathcal{F}_{\ell,p}(\rho, \phi) e^{ik_z z} \quad (1)$$

where carets denote unit vectors, k_z is the axial wavevector with the light travelling along the $+z$ axis and $\mathcal{F}_{\ell,p}$ is the mode function which includes both the amplitude and phase functions in terms of the plane-polar coordinates (ρ, ϕ) . The mode is labelled by the indices ℓ and p , with ℓ the winding number and p could be an azimuthal number, as in the case of Laguerre-Gaussian (LG) optical vortex modes, or could be redundant, as in the case of optical Bessel modes, but the treatment is not restricted to LG or Bessel modes and is applicable in general for other radially-polarised paraxial optical vortex modes. In what follows, it is convenient to refer to $\hat{\rho} \mathcal{F}_{\ell,p}$ as just $\hat{\rho} \mathcal{F}$ and only revert to including the subscript ℓ, p when the need arises.

Using the standard form of the curl of a vector in cylindrical coordinates we obtain for the magnetic field $\mathbf{B}(\rho, \phi, z) = \nabla \times \mathbf{A}(\rho, \phi, z)$. With the vector potential as defined for the radially-polarised mode in Eq.(1) we obtain the paraxial magnetic field to leading order

$$\mathbf{B}(\rho, \phi, z) = ik_z \hat{\phi} \mathcal{F} e^{ik_z z} - \hat{z} \frac{1}{\rho} \frac{\partial \mathcal{F}}{\partial \phi} e^{ik_z z} \quad (2)$$

The electric field follows from the magnetic field using Maxwell's equation

$$\nabla \times \mathbf{B} = \frac{1}{c^2} \frac{\partial \mathbf{E}}{\partial t} \quad (3)$$

We obtain, to the same leading order as for the magnetic field

$$\mathbf{E}(\rho, \phi, z) = ick_z \hat{\rho} \mathcal{F} e^{ik_z z} - \hat{z} c \frac{1}{\rho} \frac{\partial (\rho \mathcal{F})}{\partial \rho} e^{ik_z z} \quad (4)$$

The general paraxial radially-polarised vector modes we are concerned with here have the following mode function

$$\mathcal{F}_{\ell,p}(\rho, \phi, z) = \tilde{\mathcal{F}}_{\ell,p}(\rho) e^{i\ell\phi} e^{ik_z z} \quad (5)$$

where we have separated the phase dependence, so now $\tilde{\mathcal{F}}_{\ell,p}$ is a radial amplitude function (as it depends on only the radial coordinate ρ). The phase function $e^{i\ell\phi}$ contains the usual azimuthal dependence as well as the Gouy and curvature phase functions. We have

$$\Phi = \ell\phi + \Theta_{Gouy} + \Theta_{curv}, \quad (6)$$

Since we are dealing with optical vortex modes the index ℓ is the familiar winding number, while m could be a radial number as for Laguerre-Gaussian modes in which case we have for the Gouy and curvature phase functions

$$\Theta_{Gouy} = -(2p+|\ell|+1) \tan^{-1}(z/z_R); \quad \Theta_{curv} = \frac{k_z \rho^2 z}{2(z^2 + z_R^2)}. \quad (7)$$

We focus on paraxial modes for which the Gouy and curvature phases are negligible, or vanishing, as on the focal plane $z = 0$ and for the case of large Rayleigh range z_R in which case we only have the phase angle $\ell\phi$ in Eq.(6). We shall first develop the analysis for a general $\tilde{\mathcal{F}}$, which could be appropriate for any optical vortex.

CYCLE-AVERAGED OPTICAL PROPERTIES

The optical vortex mode properties of significance which we shall be concerned with here are the three cycle-averaged properties, namely the optical spin angular momentum (SAM) density \bar{s} , the angular momentum (AM) density \bar{j} and the helicity density $\bar{\eta}$. These cycle-averaged densities are generally defined as follows [1, 5, 23–27]

$$\begin{aligned} \bar{s} &= \frac{1}{4\omega} \Im \left\{ [\epsilon_0 \mathbf{E}^* \times \mathbf{E}] + \frac{1}{\mu_0} [\mathbf{B}^* \times \mathbf{B}] \right\}; \\ &= \bar{s}_E + \bar{s}_B \quad (\text{SAM density}) \end{aligned} \quad (8)$$

$$\vec{j} = \mathbf{r} \times \vec{\pi}; \quad (\text{AM density}) \quad (9)$$

$$\bar{\eta}(\mathbf{r}) = \frac{c}{\omega^2} \bar{\chi} = -\frac{\epsilon_0 c}{2\omega} \Im[\mathbf{E}^* \cdot \mathbf{B}]$$

(Helicity/ Chirality density) (10)

where in the above $\vec{\pi} = \frac{1}{c^2} \vec{\mathbf{w}}$ is the linear momentum density with $\vec{\mathbf{w}} = \frac{1}{2\mu_0} \Re[\mathbf{E}^* \times \mathbf{B}]$ the energy density. The symbols $\Re[\dots]$ and $\Im[\dots]$ stand for real and imaginary parts of $[\dots]$ and the superscript $*$ in \mathbf{E}^* stands for the complex conjugate of \mathbf{E} . As stated above we deal in turn with the evaluations of above densities specifically in relation to the radially-polarised optical vortex modes. The final

tasks involve evaluating the total (integrated) properties, namely total helicity, total SAM and total angular momentum with each evaluated as the space integral of the density variations over the x-y plane.

Evaluation of SAM

We begin with the evaluation of the spin angular momentum density. We have for the electric field part $\bar{\mathbf{s}}_E$

$$\bar{\mathbf{s}}_E = \frac{\epsilon_0}{4\omega} \Im[\mathbf{E}^* \times \mathbf{E}] \quad (11)$$

Substituting for the electric fields, we have

$$\begin{aligned} \bar{\mathbf{s}}_E &= \frac{\epsilon_0}{4\omega} \Im \left(-ick_z \hat{\rho} \mathcal{F}^* e^{-ik_z z} - \hat{\mathbf{z}} c \left\{ \frac{\mathcal{F}^*}{\rho} + \left[\frac{\partial \mathcal{F}}{\partial \rho} \right]^* \right\} e^{-ik_z z} \right) \times \left(ick_z \hat{\rho} \mathcal{F} e^{ik_z z} - \hat{\mathbf{z}} c \left\{ \frac{\mathcal{F}}{\rho} + \frac{\partial \mathcal{F}}{\partial \rho} \right\} e^{ik_z z} \right) \quad (12) \\ &= -\frac{c^2 k \epsilon_0}{2\omega} \left(\frac{|\tilde{\mathcal{F}}|^2}{\rho} + \tilde{\mathcal{F}}^* \tilde{\mathcal{F}}' \right) \hat{\phi} \\ &= -\frac{c^2 k \epsilon_0}{2\omega} \left(\frac{|\tilde{\mathcal{F}}|^2}{\rho} + \tilde{\mathcal{F}}^* \tilde{\mathcal{F}}' \right) (-\sin \phi \hat{\mathbf{x}} + \cos \phi \hat{\mathbf{y}}) \quad (13) \end{aligned}$$

Thus we have found that the electric field part of the SAM density of a radially-polarised optical vortex mode is oriented azimuthally, so has both x - and y - compo-

nents which vary with ϕ .

Consider next the magnetic field contribution $\bar{\mathbf{s}}_B = \frac{1}{4\omega\mu_0} \Im[\mathbf{B}^* \times \mathbf{B}]$. We have

$$\begin{aligned} \bar{\mathbf{s}}_B &= \frac{1}{4\mu_0\omega} \Im \left\{ \left(-ik_z \hat{\phi} \mathcal{F}^* e^{-ik_z z} - \hat{\mathbf{z}} \frac{1}{\rho} \left[\frac{\partial \mathcal{F}}{\partial \phi} \right]^* e^{-ik_z z} \right) \times \left(ik_z \hat{\phi} \mathcal{F} e^{ik_z z} - \hat{\mathbf{z}} \frac{1}{\rho} \left[\frac{\partial \mathcal{F}}{\partial \phi} \right] e^{ik_z z} \right) \right\} \\ &= \Im \left(\frac{ik_z}{4\mu_0\omega\rho} \right) \left[\mathcal{F}^* \left(\frac{\partial \mathcal{F}}{\partial \phi} \right) + \mathcal{F} \left(\frac{\partial \mathcal{F}}{\partial \phi} \right)^* \right] \hat{\phi} \times \hat{\mathbf{z}} = \mathbf{0} \quad (14) \end{aligned}$$

The last equality follows once we evaluate the angular derivatives. Thus the magnetic field contribution to the SAM density is zero and we have only the electric field contribution $\bar{\mathbf{s}}_E$, given by Eq.(13).

The total (space-integrated) SAM vanishes identically

$$\bar{\mathbf{S}} = \int_0^{2\pi} d\phi \int_0^\infty \rho d\rho [\bar{\mathbf{s}}_E + \bar{\mathbf{s}}_B] = \mathbf{0}; \quad (15)$$

where each of the x - and y - components of the SAM density yields a zero result by virtue of the angular integration.

Evaluation of angular momentum

Next we evaluate the cycle-averaged angular momentum density of the radially-polarised vortex which is given by

$$\vec{j} = \mathbf{r} \times \vec{\pi} = \frac{1}{2c^2\mu_0} [\mathbf{r} \times (\Re[\mathbf{E}^* \times \mathbf{B}])] \quad (16)$$

Consider the cross product in Eq.(16) which we evaluate as follows

$$\begin{aligned}
\mathbf{E}^* \times \mathbf{B} &= \left(-ick_z \hat{\rho} \mathcal{F}^* e^{-ik_z z} - \hat{z} c \left\{ \frac{\mathcal{F}^*}{\rho} + \left[\frac{\partial \mathcal{F}}{\partial \rho} \right]^* \right\} e^{-ik_z z} \right) \times \left(ik_z \hat{\phi} \mathcal{F} e^{ik_z z} - e^{ik_z z} \hat{z} \frac{\partial \mathcal{F}}{\rho \partial \phi} \right) \\
&= ick_z \left(\frac{|\tilde{\mathcal{F}}|^2}{\rho} + \tilde{\mathcal{F}} \tilde{\mathcal{F}}' \right) \hat{\rho} + \left\{ \ell ck_z \frac{|\tilde{\mathcal{F}}|^2}{\rho} \right\} \hat{\phi} + k_z^2 c |\tilde{\mathcal{F}}|^2 \hat{z}
\end{aligned} \tag{17}$$

Therefore on taking the real part, we have

$$\Re[\mathbf{E}^* \times \mathbf{B}] = k_z c \ell \frac{|\tilde{\mathcal{F}}|^2}{\rho} \hat{\phi} + k_z^2 c |\tilde{\mathcal{F}}|^2 \hat{z} \tag{18}$$

The angular momentum density follows

$$\begin{aligned}
\bar{\mathbf{j}} &= \frac{1}{2c^2 \mu_0} \mathbf{r} \times \Re[\mathbf{E}^* \times \mathbf{B}] \\
&= \left(\frac{k_z}{2c\mu_0} \right) \{ \rho \hat{\rho} \} \times \left\{ \ell \frac{|\tilde{\mathcal{F}}|^2}{\rho} \hat{\phi} + k_z |\tilde{\mathcal{F}}|^2 \hat{z} \right\} \\
&= \left(\frac{k_z}{2c\mu_0} \right) \left\{ \ell |\tilde{\mathcal{F}}|^2 \hat{z} - k_z |\tilde{\mathcal{F}}|^2 \rho \hat{\phi} \right\}
\end{aligned} \tag{19}$$

Since we have $\hat{\phi} = -\hat{x} \sin \phi + \hat{y} \cos \phi$ the angular momentum density vector has all three Cartesian components. However, the transverse (x - and y -) components are ϕ -dependent and, as we point out shortly, will result in zero on angular integration.

Once again we consider the total angular momentum as the space integral of the angular momentum density.

$$\bar{\mathcal{J}} = \int_0^{2\pi} d\phi \int_0^\infty \rho d\rho \bar{\mathbf{j}} \tag{20}$$

The x - and y - components give zero each due to vanishing angular integration. We are left only with the z -component, so we have

$$\bar{\mathcal{J}} = \hat{z} \ell \left(\frac{k_z \pi}{c\mu_0} \right) I_P \tag{21}$$

where the integral I_P is related to the applied power \mathcal{P} of the mode, evaluated as the space integral over the beam cross-section of the z -component of the Poynting vector. We have

$$\mathcal{P} = \frac{1}{2\mu_0} \int_0^{2\pi} d\phi \int_0^\infty |(\mathbf{E}^* \times \mathbf{B})_z| \rho d\rho \tag{22}$$

with

$$(\mathbf{E}^* \times \mathbf{B})_z = ck_z^2 |\tilde{\mathcal{F}}|^2 \tag{23}$$

We can then write for I_P

$$I_P = \int_0^\infty |\tilde{\mathcal{F}}|^2 \rho d\rho \tag{24}$$

Thus we obtain for the power \mathcal{P}

$$\mathcal{P} = \left(\frac{\pi ck_z^2}{\mu_0} \right) I_P \tag{25}$$

Substituting for I_P , we have for the total angular momentum per unit length

$$\bar{\mathcal{J}} = \ell \mathcal{L}_0 \hat{z} \tag{26}$$

where \mathcal{L}_0 has the dimensions of angular momentum per unit length and is given by

$$\mathcal{L}_0 = \left(\frac{\mathcal{P}}{k_z c^2} \right) \tag{27}$$

Thus we find that $\bar{\mathcal{J}}$ is axial and proportional to ℓ which confirms that the angular momentum carried by the radially-polarised LG mode is purely an orbital angular momentum. Note that we have determined the angular momentum without specifying the type of mode. The result is therefore general and it agrees with the result for linearly-polarised Laguerre-Gaussian light [28]. There is no contribution to be associated with spin angular momentum, which we have already confirmed to be zero.

Evaluation of helicity and chirality

In optical physics, the properties of helicity and chirality are such that two optical modes which differ only in the sign of the winding number ℓ are distinguishable. In that case, one beam is a phase-inverted mirror image of the other beam. Such kind of optical mode is then said to exhibit chirality which has been a subject of considerable investigation [27, 29–34]. More recent investigations have spurred interest in chirality which include the references [16, 23, 35–39].

The cycle averages of helicity density $\bar{\eta}$ and chirality density $\bar{\chi}$ are proportional to each other, as in Eq.(10). It is for this reason that only the helicity is discussed. In general when a light field is shown to possess helicity, it also has a corresponding chirality and we say the light is chiral, which here means if there is a change in the sign of the winding number the signs of both the helicity and the chirality change.

In their recent work, Nechayev et al [16] suggested that there exist two kinds of chirality. The first is non-geometrical which includes optical chirality due to elliptical polarisation and the second, which is termed the

Kelvin chirality, depends on the geometrical structure of the mode. This work followed the experiment by Wozniak et al [38] in which linearly-polarised Laguerre-Gaussian modes were shown to display chirality. Here we seek to evaluate the chirality density and its space integral and aim to find out whether the chirality of radially-polarised optical modes can be classed as Kelvin chirality,

or is it the usual optical non-geometrical chirality.

We begin by considering helicity, rather than chirality, as the two differ by a proportionality factor [40]. The cycle-averaged helicity density of the radially-polarised mode is as defined generally in Eq.(10). Substituting for the fields using Eqs.(2) and (4), we have for the dot product

$$\begin{aligned} [\mathbf{E}^* \cdot \mathbf{B}] &= \left\{ -ick_z \hat{\rho} \mathcal{F}^* e^{-ik_z z} - \hat{z} c \frac{1}{\rho} \left(\frac{\partial(\rho \mathcal{F})}{\partial \rho} \right)^* e^{-ik_z z} \right\} \cdot \left\{ ik_z \hat{\phi} \mathcal{F} e^{ik_z z} - \hat{z} \frac{1}{\rho} \frac{\partial \mathcal{F}}{\partial \phi} e^{ik_z z} \right\} \\ &= c \frac{1}{\rho^2} \left(\frac{\partial(\rho \mathcal{F})}{\partial \rho} \right)^* \left(\frac{\partial \mathcal{F}}{\partial \phi} \right) \\ &= \frac{ic\ell}{\rho^2} \left(\frac{\partial(\rho \tilde{\mathcal{F}})}{\partial \rho} \right)^* \tilde{\mathcal{F}} = i\ell c \left[\frac{1}{\rho} \tilde{\mathcal{F}}'^* \tilde{\mathcal{F}} + \frac{1}{\rho^2} |\tilde{\mathcal{F}}|^2 \right] \end{aligned} \quad (29)$$

where $\tilde{\mathcal{F}}' = d\tilde{\mathcal{F}}/d\rho$. Noting that $\tilde{\mathcal{F}}$ is real, we have for the helicity density of the radially-polarised general vortex mode

$$\bar{\eta}(\mathbf{r}) = -\ell \frac{\epsilon_0 c^2}{2\omega} \left[\frac{1}{\rho} \tilde{\mathcal{F}}'^2 \tilde{\mathcal{F}} + \frac{1}{\rho^2} |\tilde{\mathcal{F}}|^2 \right] \quad (29)$$

This result is applicable to any paraxial radially-polarised optical vortex and, if required for a particular case, all we need then is to specify the amplitude function $\tilde{\mathcal{F}}$. Note that the helicity density is proportional to ℓ and so in addition to changing with the magnitude of ℓ , it also changes with the sign of ℓ , hence exhibiting the chirality feature that is common to all optical vortex modes.

Integrated Helicity

The total integral of the helicity density over the $x-y$ plane is

$$\begin{aligned} \bar{\mathcal{C}}_{\ell,p} &= -\ell \frac{\pi \epsilon_0 c^2}{\omega} \int_0^\infty \rho d\rho \left[\frac{1}{\rho} \tilde{\mathcal{F}}'_{\ell,p} \tilde{\mathcal{F}}_{\ell,p} + \frac{1}{\rho^2} |\tilde{\mathcal{F}}_{\ell,p}|^2 \right] \\ &= \mathcal{I}_1 + \mathcal{I}_2 \end{aligned} \quad (30)$$

We now show that \mathcal{I}_1 is identically zero for all $\tilde{\mathcal{F}}$. We have

$$\begin{aligned} \mathcal{I}_1 &= -\ell \frac{\epsilon_0 \pi c^2}{2\omega} \int_0^\infty \left(\frac{d}{d\rho} \tilde{\mathcal{F}}^2 \right) d\rho \\ &= -\ell \frac{\epsilon_0 \pi c^2}{2\omega} \left[\tilde{\mathcal{F}}^2(\rho) \right]_0^\infty \\ &= 0 \end{aligned} \quad (31)$$

since the $\tilde{\mathcal{F}}(0) = 0 = \tilde{\mathcal{F}}(\infty)$. We are thus left with the second term so that for any $\tilde{\mathcal{F}}$ the helicity per unit length is given by

$$\bar{\mathcal{C}}_{\ell,p} = \mathcal{I}_2 = -\ell \frac{\pi \epsilon_0 c^2}{\omega} \int_0^\infty \rho d\rho \left[\frac{1}{\rho^2} |\tilde{\mathcal{F}}_{\ell,p}|^2 \right] \quad (32)$$

This is the general expression for the total helicity per unit length of a mode of any paraxial twisted light mode that is radially-polarised. Although we are able to make definitive statements about the total SAM and total angular momentum for all forms of \mathcal{F} characterising radially-polarised twisted light, we are not able to proceed further to evaluate the total helicity in Eq.(32) without specific knowledge about the form of $\tilde{\mathcal{F}}$. In the next section we focus on the form of $\tilde{\mathcal{F}}$ appropriate for a Laguerre-Gaussian optical vortex and aim to evaluate the helicity density given by Eq.(29) and the total helicity given by Eq.(32).

APPLICATIONS TO LAGUERRE-GAUSSIAN MODES

A paraxial Laguerre-Gaussian mode of winding number ℓ , radial number p and waist w_0 has an amplitude function given by

$$\tilde{\mathcal{F}}_{\ell,p}(\rho) = \mathcal{E}_0 \sqrt{\frac{p!}{(p+|\ell|)!}} e^{-\frac{\rho^2}{w_0^2}} \left(\frac{\sqrt{2}\rho}{w_0} \right)^{|\ell|} L_p^{|\ell|} \left(\frac{2\rho^2}{w_0^2} \right) \quad (33)$$

where \mathcal{E}_0 is a normalisation factor and we have identified m as the radial number p in LG modes. The factor \mathcal{E}_0 is determined in terms of the applied power \mathcal{P} of the mode which we have already evaluated above in terms of the integral I_P . For a Laguerre-Gaussian mode the integral in (24) is standard and gives

$$I_P = \int_0^\infty |\tilde{\mathcal{F}}|^2 \rho d\rho = \frac{1}{4} \mathcal{E}_0^2 w_0^2 \quad (34)$$

and so we can now determine the overall factor \mathcal{E}_0 for the Laguerre-Gaussian beam. We have

$$\mathcal{E}_0^2 = \frac{4\mathcal{P}}{\pi\epsilon_0 c^3 k_z^2 w_0^2} \quad (35)$$

Consider first the variations of the helicity density for representative modes, namely $\ell = 1, 2$. The general expression for the helicity density Eq.(29) is circularly-symmetric as it is a function only of the radial coordinate ρ . For a LG mode, we simply substitute for $\tilde{\mathcal{F}}$ given by Eq.(33) and we obtain the variation of the helicity density, as shown in Fig. 1 for $\ell = 1$ and Fig. 2 for $\ell = 2$. The plots in each case show the contributions from the first term, the second term and their sum. Confirmation of the vanishing integral of the first term are shown in Figs. 3 for $\ell = 1$ and Fig.4 for $\ell = 2$ where the areas under the curves corresponding to the areas enclosed by the integrands due to the first term are zero for both $\ell = 1$ and $\ell = 2$. We have confirmed that the variations shown for the case $\ell = 2$ define the trend for $\ell > 2$

Note, in particular, that the variations of the helicity density for the case $\ell = 1$, shown in Fig. 1 differ significantly from those of $\ell \geq 2$ in Fig.2, primarily in that the helicity density does not vanish at the core where $\rho = 0$ for $\ell = 1$, while it does vanish at $\rho = 0$ for $\ell \geq 2$. This behaviour can be explained by inspecting the general form of the helicity density Eq.(29). When applied to the Laguerre-Gaussian \mathcal{F} for $\ell = 1$, we have from Eq.(33)

$$\tilde{\mathcal{F}}_{\ell=1} \propto \rho e^{-\rho^2/w_0^2} L_p^1 \left(\frac{2\rho^2}{w_0^2} \right) \quad (36)$$

Hence

$$|\tilde{\mathcal{F}}_{\ell=1}|^2 \propto \rho^2 e^{-2\rho^2/w_0^2} \left[L_p^1 \left(\frac{2\rho^2}{w_0^2} \right) \right]^2 \quad (37)$$

Also, since \mathcal{F}' does not vanish at $\rho = 0$ we can write

$$[\tilde{\mathcal{F}}'\tilde{\mathcal{F}}]_{\ell=1} \propto \rho e^{-\rho^2/w_0^2} L_p^1 \left(\frac{2\rho^2}{w_0^2} \right) \tilde{\mathcal{F}}'_{\ell=1} \quad (38)$$

When substituted in the helicity density expression Eq.(29) we see that the $1/\rho$ in the first term cancels with the factor ρ in the numerator. Similarly the factor $1/\rho^2$ in the second term cancels the factor ρ^2 in the numerator of the second term. The overall variation amounts to a non zero value of the helicity at $\rho = 0$ only in the case $\ell = 1$. This variation contrasts with the case $\ell \geq 2$ in which the numerators in the two terms have higher powers of ρ , always guaranteeing that the helicity density vanishes at $\rho = 0$.

It is straightforward to proceed to evaluate the helicity per unit length for $\tilde{\mathcal{F}}$ corresponding to a Laguerre-Gaussian mode. Using the integration variable $x =$

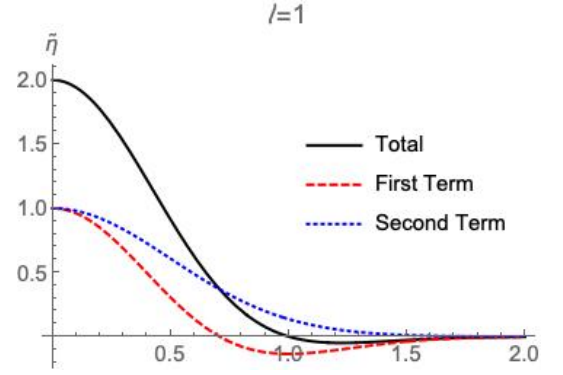


FIG. 1: Variation with the radial coordinate ρ (in units of the beam waist w_0) of the helicity density due to LG modes for which (a) $\ell = 1$. The dashed red curve shows the contribution of the first term in Eq.(29) involving the derivative $\tilde{\mathcal{F}}'$. The blue dotted curve represents the contribution of the second term and the solid black curve is the sum. Note in particular that for $\ell = 1$ the helicity density does not vanish at the core $\rho = 0$

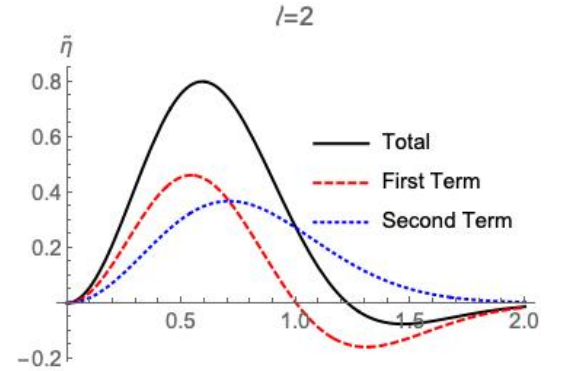


FIG. 2: The case of LG mode with $\ell = 2$. Variation with the radial coordinate ρ (in units of the beam waist w_0) of the helicity density due to LG modes for which (a) $\ell = 2$. The dashed red curve shows the contribution of the first term in Eq.(29) involving the derivative $\tilde{\mathcal{F}}'$. The blue dotted curve represents the contribution of the second term and the solid black curve is the sum. Note in particular that for $\ell = 2$ the helicity density vanishes at the core $\rho = 0$

$2\rho^2/w_0^2$ we have

$$\begin{aligned} \bar{\mathcal{C}}_{\ell,p} &= -\ell \frac{\pi\epsilon_0 c^2}{\omega} \mathcal{E}_0^2 \frac{p!}{2(p+|\ell|)!} \int_0^\infty x^{|\ell|-1} e^{-x} [L_p^{|\ell|}(x)]^2 dx \\ &= -\ell \frac{\pi\epsilon_0 c^2}{\omega} \mathcal{E}_0^2 \frac{1}{2|\ell|} \end{aligned} \quad (39)$$

The details of the evaluation of the integral in Eq.(39)

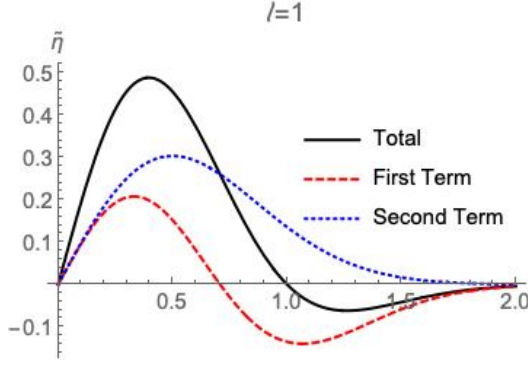


FIG. 3: The case of LG mode with $\ell = 1$. Variations of the helicity density integrand terms in \mathcal{I}_1 and \mathcal{I}_2 , (defined in Eq.(30)) with the radial coordinate (in units of w_0). The area enclosed by each curve corresponds to the contribution of the term to the total (integrated) helicity. The area enclosed by the dashed red curve is verified to be zero, consistent with Eq.(31).

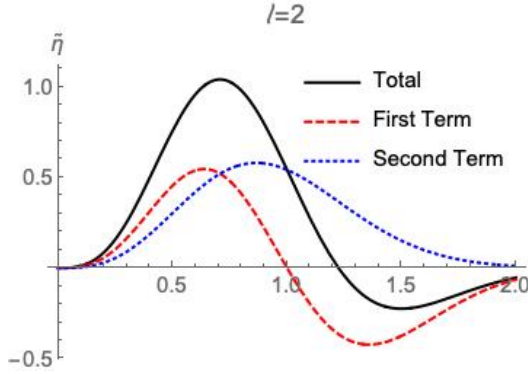


FIG. 4: The case of LG mode with $\ell = 2$. Variations of the helicity density integrand terms in \mathcal{I}_1 and \mathcal{I}_2 , (defined in Eq.(30)) with the radial coordinate (in units of w_0). The area enclosed by each curve corresponds to the contribution of the term to the total (integrated) helicity. The area enclosed by the dashed red curve is verified to be zero, consistent with Eq.(31).

are shown in Appendix A. We now have

$$\begin{aligned} \bar{\mathcal{C}}_{\ell,p} &= -\frac{\mathcal{E}_0^2 \pi \epsilon_0 c^2}{2\omega} \frac{\ell}{|\ell|} \\ &= -\left(\frac{\ell}{|\ell|}\right) \left(\frac{\mathcal{P}}{k_z c^2}\right) \left\{ \frac{2}{k_z^2 w_0^2} \right\} \\ &= \pm \mathcal{L}_0 \left\{ \frac{2}{k_z^2 w_0^2} \right\} \end{aligned} \quad (40)$$

where \mathcal{L}_0 is the constant angular momentum per unit length as defined in Eq.(27) for a fixed power \mathcal{P} and we have substituted for \mathcal{E}_0 using Eq.(35). Note that this result is independent of p and clearly depends only on the sign (not the magnitude) of ℓ . We know that the mode is not circularly polarised, but we have found that

the total helicity is similar to, but not the same as, that of circular polarisation, characterised by the pre-factor $\sigma = \pm 1$. It is easy to check that the helicity has the dimensions of angular momentum per unit length, but the factor $1/k_z^2 w_0^2$ is small for $w_0^2 \gg 1/k_z^2$ (which amounts to $w_0 \gg \bar{\lambda}$ where $\bar{\lambda} = \lambda/2\pi$ is a reduced wavelength). Thus the helicity is significant in the case of LG beams only for small beam waists w_0 and diminishes for progressively larger w_0 .

COMMENTS AND CONCLUSIONS

Our primary aim in this paper involved the derivation of the optical properties of paraxial radially-polarised twisted light modes, namely the spin orbital angular momentum (SAM), the total angular momentum (which is formally the sum of spin and orbital angular momentum for paraxial light), and their helicity and chirality. We set out to keep the type of mode unspecified and arrived at the results for the angular momentum and SAM, but for the helicity we are able to arrive at general results and applied them to the Laguerre-Gaussian modes as a specific case. Our treatment is based on general expressions describing the radially-polarised electric and magnetic fields which incorporate the longitudinal component and which were subject to verification of Maxwell's consistency conditions, namely that the electric field in Cartesian coordinates follows from a derived expression of the magnetic field using the Maxwell curl equation, also in Cartesian coordinates, and the magnetic field follows from the electric field using the other Maxwell curl equation. The final Cartesian expressions are then presented in cylindrical polar coordinates. We have checked that the formalism presented is verifiable to leading order in the paraxial approximation.

We have found that in general, the radially-polarised twisted light modes exhibit only cycle-averaged transverse SAM components, which arise entirely from the electric field part, are ϕ -dependent, while the magnetic field contribution to the SAM density is shown to be identically zero. The space integral of the SAM density leading to the total SAM is therefore zero. Thus we have confirmed that in general such radially-polarised modes have no SAM. Next we evaluated the angular momentum, which, for paraxial modes, is always the sum of the spin angular momentum and the orbital angular momentum and we have found that the angular momentum density is proportional to the winding number ℓ , indicating that this contribution of the total angular momentum density is purely orbital, but there are also transverse density components which, like the SAM density case, depend on ϕ and so lead to zero on spatial integration. The integrated total angular momentum is also proportional to ℓ and so purely orbital in origin. This result is consistent with the SAM result which was evaluated independently,

that the mode has no SAM.

The helicity density evaluations could also be carried out for a general radially-polarised optical vortex mode characterised by an unspecified $\tilde{\mathcal{F}}$ with the density and the general results for the helicity density and the total (integrated) helicity we arrived at are shown in Eq.(29) for the helicity density and in Eq.(32) for the integrated helicity. We proceeded to explore the helicity density variations for the spacial cases of Laguerre-Gaussian modes and pointed out the special behaviour for $\ell = 1$ in that the helicity density does not vanish at $\ell = 1$ at the core $\rho = 0$, while it does vanish for all $\ell \geq 2$. We explained this behaviour by inspecting the ρ variations of the two terms in the helicity density, confirming that for $\ell = 1$ the helicity density has overall dependence ρ^0 and so the helicity density does not vanish at $\rho = 0$ for $\ell = 1$.

Finally, we evaluated the total helicity of the radially-

polarised Laguerre-Gaussian optical vortex and found it equal to $(\ell/|\ell|)\mathcal{Q} = \mathcal{N}\mathcal{Q}$, where $\mathcal{N} = \pm 1$ is interpreted as a Hopf index and \mathcal{Q} is the action constant. The ± 1 is reminiscent of $\sigma = \pm 1$ for circular polarisation. This result holds for any radially-polarised LG mode however large the magnitude of its winding number ℓ is, but the action constant \mathcal{Q} and consequently the helicity are significant only for small beam waist w_0 and diminish for all such LG modes of large w_0 . Since this type of helicity (and chirality) originate from the spatial structure of the radially-polarised mode, they can be categorised as of the Kelvin type [16].

Disclosures

The authors declare no conflicts of interest.

APPENDIX A

We evaluate the integral in Eq.(39) which is

$$\mathcal{I} = \int_0^\infty x^{|\ell|-1} e^{-x} [L_p^{|\ell|}(x)]^2 dx \quad (41)$$

Consider the evaluation of following derivative of the function $x^{|\ell|} e^{-x} [L_p^{|\ell|}(x)]^2$ with respect to x

$$\frac{d}{dx} \{x^{|\ell|} e^{-x} [L_p^{|\ell|}(x)]^2\} = |\ell| x^{|\ell|-1} e^{-x} [L_p^{|\ell|}(x)]^2 - x^{|\ell|} e^{-x} [L_p^{|\ell|}(x)]^2 - 2x^{|\ell|} e^{-x} L_p^{|\ell|}(x) L_{p-1}^{|\ell|+1}(x) \quad (42)$$

So we may now write

$$\begin{aligned} \mathcal{I} &= \int_0^\infty x^{|\ell|-1} e^{-x} [L_p^{|\ell|}(x)]^2 dx \\ &= \frac{1}{|\ell|} \int_0^\infty \left(\frac{d}{dx} \{x^{|\ell|} e^{-x} [L_p^{|\ell|}(x)]^2\} + x^{|\ell|} e^{-x} [L_p^{|\ell|}(x)]^2 + 2x^{|\ell|} e^{-x} L_p^{|\ell|}(x) L_{p-1}^{|\ell|+1}(x) \right) dx \\ &= \frac{1}{|\ell|} \left([x^{|\ell|} e^{-x} (L_p^{|\ell|}(x))^2]_0^\infty + \int_0^\infty x^{|\ell|} e^{-x} [L_p^{|\ell|}(x)]^2 dx + 2 \int_0^\infty x^{|\ell|} e^{-x} L_p^{|\ell|}(x) L_{p-1}^{|\ell|+1}(x) dx \right) \end{aligned} \quad (43)$$

where we have integrated by parts in the derivative term. The first term in the last equality is zero on applying the integration limits, while the third term is the standard orthogonality integral of the associated Laguerre functions and so vanishes as well. We are thus left with

ACKNOWLEDGEMENTS

The authors wish to thank Professors S. Franke-Arnold, K.D. Dholakia, M. Mansuripur, E.J. Galvez, Q. Zhan, G. Milione and P. Banzer for useful correspondence.

$$\mathcal{I} = \frac{1}{|\ell|} \int_0^\infty x^{|\ell|} e^{-x} [L_p^{|\ell|}(x)]^2 dx = \frac{1}{|\ell|} \frac{(p+|\ell|)!}{p!} \quad (44)$$

- [1] L. Allen, M. Padgett, and M. Babiker, Progress in optics **39**, 291 (1999).

- [2] L. Allen, S. M. Barnett, and M. J. Padgett, *Optical Angular Momentum* (IOP Publishing, 2003).
- [3] Q. Zhan, Opt. Express **12**, 3377 (2004).
- [4] S. Franke-Arnold, L. Allen, and M. Padgett, Laser & Photonics Reviews **2** (2008).
- [5] D. L. Andrews and M. Babiker, eds., *The Angular Momentum of Light* (Cambridge University Press, Cambridge, 2012).
- [6] J. P. Torres and E. L. Torner, *Twisted photons* (Wiley-VTH, 2011).
- [7] M. Babiker, D. L. Andrews, and V. E. Lembessis, Journal of Optics **21**, 013001 (2018).
- [8] B. M. Holmes and E. J. Galvez, Journal of Optics **21**, 104001 (2019).
- [9] Y. Mushiake, K. Matsumura, and N. Nakajima, Proceedings of the IEEE **60**, 1107 (1972).
- [10] Y. Kozawa and S. Sato, Opt. Lett. **30**, 3063 (2005).
- [11] Q. Zhan, Adv. Opt. Photon. **1**, 1 (2009).
- [12] Y. Kozawa and S. Sato, J. Opt. Soc. Am. A **24**, 1793 (2007).
- [13] R. Dorn, S. Quabis, and G. Leuchs, Physical Review Letters **91**, 1 (2003).
- [14] M. Bashkansky, D. Park, and F. K. Fatemi, Opt. Express **18**, 212 (2010).
- [15] U. Levy, Y. Silberberg, and N. Davidson, Adv. Opt. Photon. **11**, 828 (ts).
- [16] S. Nechayev, J. S. Eismann, R. Alaei, E. Karimi, R. W. Boyd, and P. Banzer, Phys. Rev. A **103**, L031501 (2021).
- [17] <https://www.thorlabs.com>, <http://www.arcoptix.com>.
- [18] Porfirev, A.P., Ustinov, A.V. & Khonina, S.N. Polarization conversion when focusing cylindrically-polarized vortex beams. Sci Rep **6**, 6 (2016). <https://doi.org/10.1038/s41598-016-0015-2>.
- [19] M. Neugebauer, T. Bauer, A. Aiello, and P. Banzer, Phys. Rev. Lett. **114**, 063901 (2015).
- [20] F. Bouchard, N. H. Valencia, F. Brandt, R. Fickler, M. Huber, and M. Malik, Opt. Express **26**, 31925 (2018).
- [21] J. Hu, S. Kim, C. Schneider, S. Höfling, and H. Deng, Phys. Rev. Appl. **14**, 044001 (2020).
- [22] S. Frank-Arnold; private correspondence.
- [23] K. A. Forbes and G. A. Jones, Journal of Optics **23**, 115401 (2021).
- [24] K. A. Forbes, Phys. Rev. A **105**, 023524 (2022).
- [25] A. Aiello, P. Banzer, M. Neugebauer, and G. Leuchs, Nature Photonics **9**, 789 (2015).
- [26] K. Y. Bliokh and F. Nori, Phys. Rev. A **83**, 021803 (2011).
- [27] R. P. Cameron, S. M. Barnett, and A. M. Yao, New Journal of Physics **14**, 053050 (2012).
- [28] K. Koksai, M. Babiker, V. E. Lembessis, and J. Yuan, J. Opt. Soc. Am. B **39**, 459 (2022).
- [29] A. F. Rañada, letters in mathematical physics **18**, 97 (1989).
- [30] A. F. Rañada and J. Trueba, Physics Letters A **202**, 337 (1995).
- [31] A. Ranada and J. Trueba, Nature **384**, 124 (1996).
- [32] Y. Tang and A. E. Cohen, Phys. Rev. Lett. **104**, 163901 (2010).
- [33] I. Fernandez-Corbaton, X. Zambrana-Puyalto, and G. Molina-Terriza, Physical Review A **86**, 042103 (2012).
- [34] G. Afanasiev and Y. P. Stepanovsky, Il Nuovo Cimento A (1965-1970) **109**, 271 (1996).
- [35] K. Y. Bliokh, A. Y. Bekshaev, and F. Nori, Phys. Rev. Lett. **119**, 073901 (2017).
- [36] F. Crimin, N. Mackinnon, J. Götte, and S. Barnett, Applied Sciences **9**, 828 (2019).
- [37] F. Crimin, N. Mackinnon, J. Götte, and S. Barnett, Journal of Optics **21**, 094003 (2019).
- [38] P. Woźniak, I. De Leon, K. Höfling, G. Leuchs, and P. Banzer, Optica **6**, 961 (2019).
- [39] V. E. Lembessis, K. Koksai, J. Yuan, and M. Babiker, Phys. Rev. A **103**, 013106 (2021).
- [40] K. Koksai, M. Babiker, V. E. Lembessis, and J. Yuan, J. Opt. Soc. Am. B **39**, 459 (2022).